The Influence of Carbon Nanotube Aspect Ratio on Thermal Conductivity Enhancement in Nanotube–Polymer Composites

Rahul S. Kapadia
e-mail: rskapadi@ucsd.edu

Brian M. Louie
e-mail: bmlouie@ucsd.edu

Prabhakar R. Bandaru
Professor
e-mail: pbandaru@ucsd.edu

Department of Mechanical Engineering,
University of California,
San Diego, CA 92093

We report and model a linear increase in the thermal conductivity (κ) of polymer composites incorporated with relatively low length/diameter aspect ratio multiwalled carbon nanotubes (CNTs). There was no evidence of percolation-like behavior in the κ, at/close to the theoretically predicted threshold, which was attributed due to the interfacial resistance between the CNT and the polymer matrix. Concomitantly, the widely postulated high thermal conductivity of CNTs does not contribute to the net thermal conductivity of the composites. Through estimating the interfacial resistance and the thermal conductivity of the constituent CNTs, we conclude that our experimental and modeling approaches can be used to study thermal transport behavior in nanotube–polymer composites. [DOI: 10.1115/1.4025047]

Keywords: carbon nanotubes, filled polymers, nanocomposites, percolation, thermal conductivity, effective medium theory, thermal interface resistance, and kaptiza resistance

1 Introduction

CNTs are considered an excellent choice for fillers in polymers, e.g., over that of conventional fillers, such as carbon black particles [1], due to (a) inherently superior mechanical, electrical, and thermal properties, as well as (b) their large length (L) to diameter (d) aspect ratio (AR), which could enable reinforcement, through connectivity at a smaller volume [2]. Consequently, the mechanical attributes of polymers could still be retained, while bringing forth a significant modulation of the physical properties through composite formation. Consequently, such nanotube–polymer composites have been advocated for a variety of applications, including, thermoelectrics [3], electromagnetic shielding [4,5], electronic packaging [6], thermal metamaterials [7], etc.

It has previously been concluded by Shenogina et al. [8] through theoretical analysis (based on the finite element method (FEM) and molecular dynamics) that the low thermal conductivity (κ) contrast (of less than 10^4) between the matrix and the filler precludes a strong percolation threshold effect. A linear variation of the thermal conductivity with volume fraction was consequently predicted based on effective medium theory [9]. While the interfacial resistance between fibers and matrix was considered, the value was an order of magnitude higher than the experimentally determined values (around $7.5 \times 10^8 (\mathrm{m^2K})/\mathrm{W}$ from Huxtable et al. [10] and our results), which may have precluded the observation of percolation.

Single-walled carbon nanotube (SWCNT)-epoxy composites were studied in Biercuk et al. [11], where the SWCNTs were reported to be oriented randomly. An increase in κ was the reported as a function of added SWNT weight content with a 125% increase at 1 wt. % SWCNTs. The random orientation was thought to be the reason for the κ increase at a lower weight percentage compared to previous studies where the nanotubes were aligned perpendicular to the direction of current flow. However, the effects of interfacial resistance between the nanotubes were not considered, as will be done in our paper.

While an increase in the thermal conductivity in the nanotube–polymer composites was observed in Bonnet et al. [12] a percolation threshold was not observed. Instead, after subtracting the contribution of the polymer matrix (PMMA in their case), the conductivity variation was fit to a scaling law. A major issue with this paper is that it does not again consider the influence of the interfacial resistance. A thermal conductivity contrast ratio of 10 between the filler and the matrix was thought to be adequate for observing percolation related effects. The fits of our data to their model equation implied a thermal conductivity of $\sim$1.3 W/(m K) for the carbon nanotubes, orders of magnitude smaller than what is commonly accepted.

While a variety of techniques have been used for the experimental measurement of the thermal conductivity (κ) of nanostructure incorporated polymer composites, either steady state or transient 3ω-based techniques [13] seem to be most common. In this paper, we report results obtained through the use of the former methodology.

The notable contribution of our work consists in the investigation of a particular aspect of nanotube geometry, i.e., aspect ratio, on the thermal conductivity enhancement of nanotube constituted polymer composites. We have then been able to show that the diameter variation and related bundling would have less of a significance compared to the length variation. Our study has also indicated the dominating influence of the nanotube–polymer interface and how the constituent temperature drop mediated through the interfacial resistance precludes thermal conductivity enhancement due to the nanotubes. We have been successful in obtaining a definitive value for the interfacial resistance, $R_{\mathrm{int}} = 9 \times 10^8 (\mathrm{m^2K})/\mathrm{W}$, in addition to verifying an increase in the κ due to increasing CNT filler content (Fig. 1).

2 Synthesis of Test Samples

Multiwalled CNTs (MWCNTs), functionalized with –COOH groups, were dispersed into a reactive ethylene terpolymer (RET; Elvaloy 4170; DuPont, Inc.) for composite synthesis. For the reported experiments, two varieties of MWCNTs with similar lengths (of $\sim$1.6 μm) with different diameters (45.0 $\pm$ 14.1 nm

Contributed by the Heat Transfer Division of ASME for publication in the Journal of Heat Transfer. Manuscript received February 28, 2013; final manuscript received July 9, 2013; published online October 25, 2013. Assoc. Editor: Oronzio Manca.

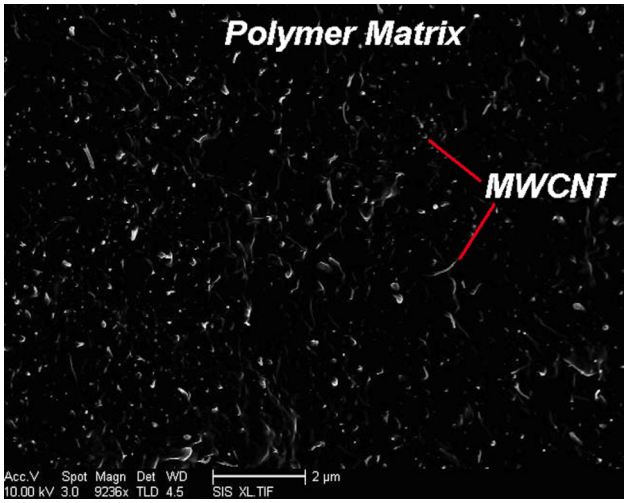

Fig. 1 Scanning electron microscope (SEM) image indicating uniform dispersion of MWCNTs in polymer matrix

and 23.0 ± 6.3 nm) leading to aspect ratios of ~35 and ~70, respectively, were used. The geometrical parameters were measured using a Philips XL30 ESEM (environmental scanning electron microscope). The particular polymer, RET, was chosen due to the presence of the epoxide constituent, which bonds with the -COOH group on the MWCNT forming robust ester-bonds, as was confirmed through Fourier-transform infrared spectroscopy (FTIR) [4,14]. For the composite synthesis, the RET was dissolved in toluene and heated at 60 °C for 2 h. The functionalized MWCNTs were also dispersed in toluene and ultrasonicated (in a Sonics VCX-750) to assure uniform mixing for 10 min. The MWCNT dispersion was then added to the RET solution and resonicated for 1 h. To remove excess solvent, the mixture was stirred for 2 h and subsequently poured in glass dish and degassed in vacuum (~1 mTorr pressure) for 12 h. We ensured the curing of the polymer through our processing treatments as per the manufacturer's recommendations. Details related to such treatments have been indicated previously by Park et al. [4]. The application of a vacuum serves for degassing of the polymer sample during the curing process. Subsequently, a hot press (from Carver, Inc.) was used to compress the composites into various thicknesses, typically of ~1.5 mm.

Composites with a maximum MWCNT filler fraction (f) ~10% were used as larger f rendered the composites brittle. However, if the f could somehow be further increased, entangling of CNTs could also occur. Consequently, we have implicitly considered that such effects are negligible. As discussed later in the paper, the relatively large extent of the interfacial layer and the magnitude of the interfacial resistance may preclude the observation of effects of nanostructure entanglement.

A uniform dispersion of the MWCNTs was recorded across the cross section of our composite (through considering SEM micrographs of sample sections at various magnifications and length scales ranging from 1 μm to 1 mm). Such homogeneous dispersion was necessary to ensure repeatable property measurements with high fidelity.

3 Steady State Heat Conductivity Measurement

We used an experimental setup following and conforming to American Society for Testing and Materials (ASTM) standards E 1225 and D 5470 [15,16], as laid out in Fig. 2. The measurements were carried out in a vacuum chamber (~5 mTorr) to minimize convective heat losses. The test composite sample was placed in between two stainless steel bars (4 cm long), with $\kappa_{SS} = 16\,W/(mK)$, fitted with three K-type thermocouples (TCs) each. A fourth TC was situated at 1 mm from the edge. Forty

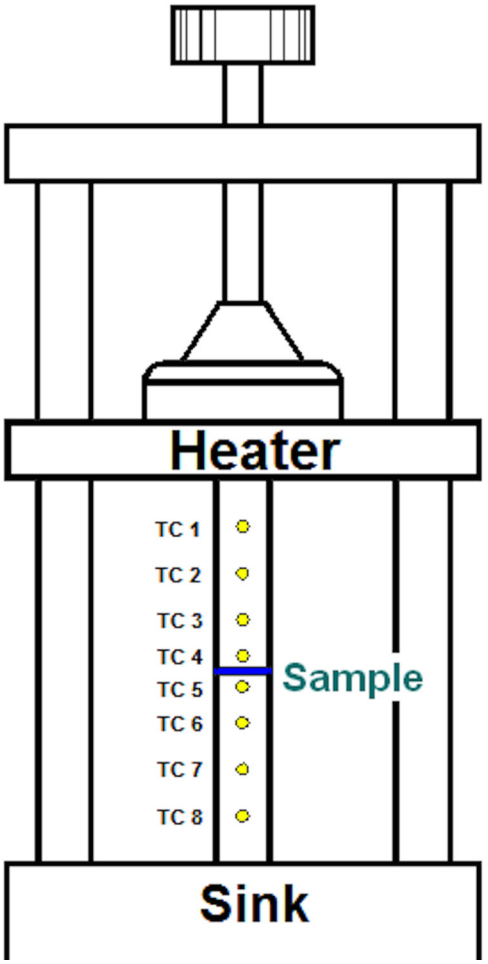

Fig. 2 Schematic representation of experimental setup for the thermal conductivity (κ) measurement of the nanotube–polymer composite. The heat flux, (q), was deduced from the TC recordings in the top and bottom stainless steel bars. Typical values of average heat flux (q_{avg}) observed was ~3500 W/m^2.

AWG gauge (0.08 mm diameter) TC wires were used to minimize the conductive heat loss. Bars were chosen with a specific length, per ASTM standards, to keep the thermal resistance (equal to the length/thermal conductivity ratio) of the bars equal to the thermal resistance of the samples, resulting in equal temperature drops across the reference bars and the sample. A cartridge heater on the top served as a heat source, while an aluminum cylinder at the bottom served as a sink. Care was taken to polish surfaces of the reference bars, in contact with the sample, to ensure good contact as well as to minimize the radiative losses. (We estimated the convective and radiative heat flux losses to be at the most 10% of the total conductive heat flux.) A uniform 15 in.-lb torque was impressed on the samples for reliable measurements. A dial gauge (with 25 μm accuracy) was used to measure the sample thickness. Steady state conditions were ensured through requiring the temperature measurement fluctuations to be less than 0.1 K over 10 min.

The above experimental configuration allowed for the assumption of a one-dimensional heat conduction equation to be employed by ensuring uniform heat source and sink and by having length of setup larger than the cross-section dimensions, from which the κ_{comp} was calculated from the sample surface temperatures T_{top} and T_{bottom} and the average heat flux q_{avg} from

$$\kappa_{comp} = q_{avg} \frac{t}{T_{top} - T_{bottom}} \tag{1}$$

The experimental setup was calibrated with Pyrex 7740 and Teflon PTFE samples, where κ was determined to be 1.14 ± 0.08 W/(m K) and 0.23 ± 0.01 W/(m K), respectively, and compares to within $\pm 5\%$ of published values [17,18].

We have taken into account both systematic and random errors in our experiment. Systematic errors arise from the TC measurements for temperatures. We take into account a 0.75% uncertainty from the specifications of our TC (from Omega, Inc.) in our temperature measurement. Using this uncertainty ($u(T)$), we then calculate the uncertainty in the heat flux ($u(q)$) in the reference bars and the extrapolated temperatures of the top and the bottom surfaces of the sample. Subsequently using these calculations, we can calculate the uncertainty in thermal conductivity ($u(\kappa)$) by the following:

$$u(\kappa) = \left(\frac{q_{\text{avg}} t}{T_{\text{top}}} u(T_{\text{top}})\right)^2 + \left(\frac{q_{\text{avg}} t}{T_{\text{bottom}}} u(T_{\text{bottom}})\right)^2 + \left(\frac{t}{T_{\text{top}} - T_{\text{bottom}}} u(T_{q_{\text{avg}}})\right)^2$$

The estimate of random errors was done through standard deviation values of measurements of three samples for each of the CNT volume fraction.

4 Results and Discussion

We observed a linear increase in κ_{comp} with increasing volume fraction of MWCNTs shown in Fig. 3. Initial understanding of such an increase was attempted, using the thermal conductivities and volume fractions of the nanotubes (CNT) and the polymer (poly) matrix (i.e., $\kappa_{\text{CNT}}, \kappa_{\text{poly}}$ and f_{CNT}, f_{poly}, respectively) through a relationship of the type: $\kappa_{\text{comp}} = \kappa_{\text{CNT}} \cdot f_{\text{CNT}} + \kappa_{\text{poly}} \cdot f_{\text{poly}}$. However, such a formulation suffers from the lack of precise knowledge of κ_{CNT} and ignores possible filler–matrix interfacial contribution. The latter would preclude the use of simple mixture rules predicated on effective medium-based approaches [19]. Using an excluded volume method [2], we calculated a critical volume fraction (f_{crit}) for percolation from

$$f_{\text{crit}} = \frac{E[V_{\text{ex}}]N_{\text{CNT}}}{\frac{4}{3} + 2\text{AR} + \frac{1}{2}\text{AR}^2}\left(\frac{1}{6} + \frac{1}{4}\text{AR}\right) \tag{2}$$

For the derivation of equation above (explained in more detail in Pfeifer et al. [2]), we used an excluded volume percolation theory based model to estimate the theoretical critical volume percolation threshold, f_{crit}, of the CNTs, as a function of L. For this, we assumed that the ith CNT has a volume, v_i, in a polymer/insulating matrix of unit volume. Now, if the percolation threshold corresponds to the connectivity of a number of CNTs ($=N_{\text{CNT}}$), then the odds of not selecting any CNT (corresponding to a point in the matrix) would be

$$(1 - f_{\text{crit}}) = (1 - v_1)\left(\frac{1 - v_1 - v_2}{1 - v_1}\right)\left(\frac{1 - v_1 - v_2 - v_3}{1 - v_1 - v_2}\right)\cdots \cdots\left(\frac{1 - v_1 - v_2 - \cdots - v_{N_{\text{CNT}}}}{1 - v_1 - v_2 - \cdots - v_{N_{\text{CNT}}-1}}\right) = 1 - N_{\text{CNT}}\sum_{i=1}^{N_{\text{CNT}}}\frac{v_i}{N_{\text{CNT}}}$$

Implying that $f_{\text{crit}} = N_{\text{CNT}}E[v]$. Here, $E[v]$ denotes the expected value or ensemble average of the CNT volume. It is to be noted that we have assumed that the CNTs were impenetrable. We then use the identity $E[v] = ((E[V_{\text{ex}}]N_{\text{CNT}})/E[V_{\text{ex}}])(E[v]/N_{\text{CNT}})$, where V_{ex} is defined as the excluded volume: the space circumscribed around the CNT by the center of another CNT, whereby both CNTs contact each other but do not overlap. For isotropically oriented, spherically capped stick like objects of diameter (d) and length (L), which we take to be akin to CNTs, $E[V_{\text{ex}}] = \frac{4\pi}{3}d^3 + 2\pi d^2 L + \frac{\pi}{2}dL^2$. In addition, for the CNT modeled as a capped cylinder, $E[v] = \frac{\pi}{6}d^3 + \frac{\pi}{4}d^2 L$. For infinitely thin cylinders of deterministic length, Monte-Carlo simulations were used to estimate $E[V_{\text{ex}}]N_{\text{CNT}}$ of $\sim$1.4 [20]. For a given aspect ratio ($\text{AR} = L/d$), the theoretical f_{crit} would then be as depicted in Eq. (2).

Consequently, we calculated $f_{\text{crit}} \sim 0.016$ ($=1.6\%$) for samples AR of 35 and for $f_{\text{crit}} \sim 0.009$ ($=0.9\%$) for AR of 70 were estimated. However, such thresholds are not apparent in the experimental observations of Fig. 3. We then sought to systematically understand the relative importance and contributions of the (a) polymer matrix, (b) polymer–CNT filler interface, and (c) the CNT geometry on κ_{comp}, to explain our findings.

It had been previously discussed by Bonnet et al. [12] that the matrix contribution could be subtracted to delineate the CNT contribution in the composite. Consequently, the difference $\Delta\kappa = \kappa_{\text{comp}} - \kappa_{\text{poly}} \cdot (1 - f)$ could be studied for observing CNT filler effects. We tried to analyze our data using this model to explain the thermal conductivity enhancement with increasing CNT filler content. With our data, as presented in Fig. 3, and plotting the $\Delta\kappa$ against $(f - f_{\text{crit}})/(1 - f_{\text{crit}})$, the thermal conductivity of the CNTs was deduced to be $\sim$1.3 W/(m K), which seemed unrealistically low. We had to then conclude that the Bonnet model, which posits percolation does not hold true for our experiments.

We suspect the possibly large contribution from the CNT–polymer interface, which may yield such low values for κ_{CNT} and preclude percolation-like phenomena. Indeed, it was previously noted [8] that the smaller thermal conductivity contrast between the CNT and polymer matrix, which could be orders of magnitude lower than the contrast in their respective electrical conductivity values, could preclude the observation of percolation. The relative contributions of the interfacial resistance would be a function of the filler geometry and, at a given volume fraction, could be more pronounced in lower AR fillers. Indeed, previous work has indicated a proportionally larger κ enhancement in polymer–CNT composites through the use of larger AR fillers [21]. A temperature drop over the interfacial layer, which for a given heat flux would yield a proportional interfacial thermal resistance R_{int} [22,23], would reduce the effective composite conductivity.

We modeled the CNT–polymer matrix interface, through a unit cell as shown in Fig. 4. Such an approach assumes that the environment around each CNT in the composite is substantially identical and may be accurate with compositions outside the percolation threshold volume fraction [9]. We also assume no heat storage in the composite or interface, a finite interfacial layer thickness, heat flux continuity across the interface, and a finite temperature discontinuity proportional to the heat flux across the interface. We employ a cylindrically shaped unit CNT, with κ_l^{cell} and κ_l^{cell} as the

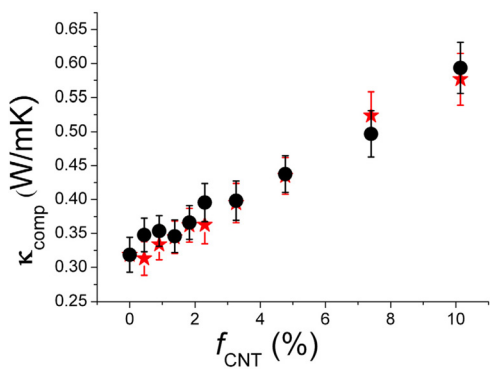

Fig. 3 Experimentally measured values of κ_{comp} with increasing volume fraction of CNTs. Circle symbols denote the values for composites with MWCNTs of AR = 35, while the star symbols denote the values for composites with MWCNTs of AR = 70.

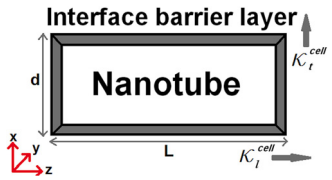

Fig. 4 A unit cell of a CNT with surrounding interface layer was used as a constituent to model the nanotube–polymer composite

equivalent thermal conductivity values along transverse (cross-sectional) and longitudinal axes. The *net* thermal resistance along this unit cell was computed through the addition of individual thermal resistances of the (i) two interfacial layers (R_{int}) on either end, together with that from the (ii) CNT, ($= L/\kappa_{\text{CNT}}$ or d/κ_{CNT}), and yields for the equivalent thermal conductivity

$$\kappa_t^{\text{cell}} = \frac{\kappa_{\text{CNT}}}{1 + \dfrac{2R_{\text{int}}}{d}\kappa_{\text{CNT}}} \tag{3}$$

$$\kappa_l^{\text{cell}} = \frac{\kappa_{\text{CNT}}}{1 + \dfrac{2R_{\text{int}}}{L}\kappa_{\text{CNT}}} \tag{4}$$

Subsequently, by following the approach of Nan [24] and Nan et al. [25], who also assumed such an effective medium-based theory, the κ_{comp} relative to the polymer matrix conductivity (κ_{poly}) was expressed using

$$\frac{\kappa_{\text{comp}}}{\kappa_{\text{poly}}} = \frac{3 + f(\beta_x + \beta_z)}{3 - f\beta_x} \tag{5}$$

where

$$\beta_x (= \beta_y) = \frac{2(\kappa_t^{\text{cell}} - \kappa_{\text{poly}})}{\kappa_t^{\text{cell}} + \kappa_{\text{poly}}} \tag{6}$$

$$\beta_z = \frac{\kappa_l^{\text{cell}}}{\kappa_{\text{poly}}} - 1 \tag{7}$$

The data shown in Fig. 5 were fitted using Eqs. (4)–(7) and yielded an R_{int} of $9 \times 10^{-8}(\text{m}^2\text{K})/\text{W}$. Such a value was comparable to the $8.3 \times 10^{-8}(\text{m}^2\text{K})/\text{W}$, estimated for single-walled CNTs encased in cylindrical micelles of sodium dodecyl sulfate surfactant [10,26] and to that calculated for SWCNTs through molecular dynamics-based simulations [27]. The R_{int} could then mask/curtail the connectivity of the CNTs. Such influence was seen through the relative insensitivity of the experimental fits (Fig. 5) to values of κ_{CNT} ranging from 50 W/(m K) to 500 W/(m K). However, we observed maximal r^2 values, of around 0.97 and 0.98 for AR 35

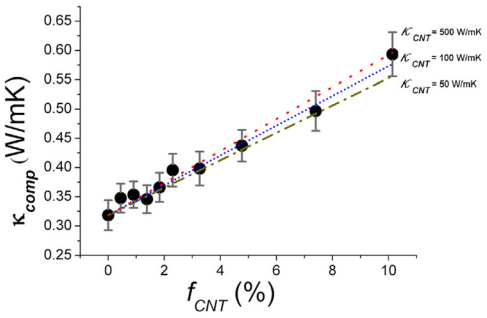

Fig. 5 Modeling κ_{comp}, using κ_{CNT} as a fitting parameter. Circle symbols indicate experimental values for composites constituted of MWCNTs with an average AR of 35.

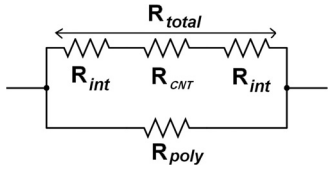

Fig. 6 Equivalent circuit model for thermal transport in a nanotube–polymer composite. The top branch indicates the two interfaces in series with a CNT, while the bottom branch models heat flow through the polymer matrix.

and AR 70, respectively, samples with a $\kappa_{\text{CNT}} = 500\,\text{W}/(\text{mK})$. Further increasing κ_{CNT} has negligible effect.

Given the close correspondence of the determined R_{int} to previous experiments and the reasonable value of κ_{CNT}, we can conclude that our approach can be used to study thermal transport behavior in nanotube–polymer composites. However, the implicit assumption of a uniform environment for all the constituent CNTs could hold only up to a certain range of CNT filler volume fraction [28]. Moreover, as discussed previously, the nanotube–polymer matrix interface, which has been posited for precluding percolation, is not explicitly considered in effective-medium theories.

To further understand the role of the interface, we propose a circuit model for thermal transport through the nanotube–polymer composite, as shown in Fig. 6. We assume two parallel paths: one through the interface/CNT/interface and another through the polymer matrix. The thermal resistance per unit area in the former path (R_{total}) is the sum of the thermal resistances of CNT (R_{CNT}) and the two interfacial resistances (R_{int}). For the polymer matrix (i.e., R_{poly}) $\sim 5 \times 10^{-6}(\text{m}^2\text{K})/\text{W}$ computed over the length of the nanotube. Through comparison of the $R_{\text{total}}/R_{\text{int}}$ ratio, with changing κ_{CNT}, it was observed that the ratio tends to 1, after a κ_{CNT} of $\sim$100 W/(m K) (Fig. 7). Consequently, we do not see any further enhancement in the value of κ_{comp} as the interface resistance is much more dominant and the CNT contribution is effectively cut off.

As it was observed, the increase of the κ_{comp} seems to be independent of AR (Fig. 3), we probed this aspect through an individual consideration of the respective lengths and diameters, which contributes to κ_l^{cell} and κ_t^{cell}, respectively (Fig. 4). Comparing the modeled κ values in Figs. 8 and 9, we see that increasing the AR of composites by increasing the length of MWCNTs has a greater effect on the increase in the κ_{comp} than by changing the diameter. This can also be attributed to the length being at least 2 orders of magnitude bigger than the diameter. Thus, comparing the experimental results to the modeled lines in Figs. 8 and 9, we see that a diameter-induced variation of the AR had less of an influence on

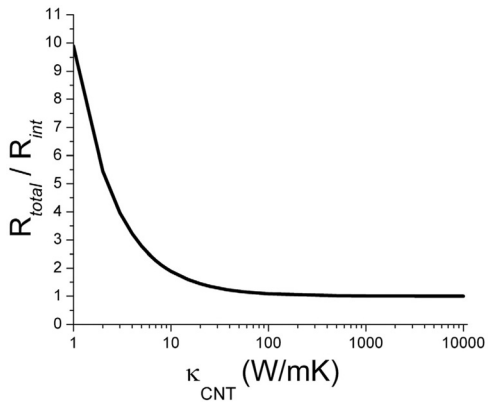

Fig. 7 Ratio of the thermal resistance from the nanotube and two interfaces: (R_{total}) to the interfacial resistance, (R_{int}), as a function of the intrinsic thermal conductivity of the CNT: κ_{CNT}

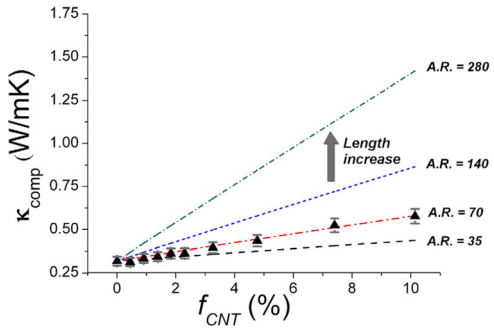

Fig. 8 Modeled κ_{comp} increase, showing effect of increasing length, *L* of MWCNT (*d* is constant). Triangle symbols indicate experimental data for composites with constituent MWCNT fillers of average AR of 70.

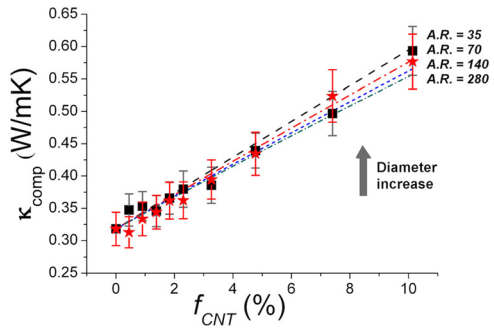

Fig. 9 Modeled κ_{comp} increase showing effect of increasing diameter, *d* of MWCNT (*L* is constant). Square symbols indicate experimental data for composites with constituent MWCNT fillers of average AR of 35, while star symbols indicate experimental data for composites with constituent MWCNT fillers of average AR of 70.

the κ_{comp} variation, in accordance with experiments. Consequently, the experimentally observed κ_{comp} would be more related to a diameter variation.

It has been previously discussed [29] that the contribution of the chemical bonding between –COOH functionalized CNTs and an epoxy resin matrix may lead to a higher enhancement in the κ with a lower thermal interfacial resistance, compared to when the CNTs were dispersed in a nonepoxy-based resin, e.g., cynate ester. However, the bond heterogeneity (i.e., the ester linkage) would yet be manifested as a finite interfacial resistance with lower κ than that of the CNTs. Such low value for R_{int} is 2 orders of magnitude lower compared to that found for vertically aligned thermally conductive functionalized multilayer graphene sheets [30], where an $R_{int} \sim 5 \times 10^{-6}(m^2K)/W$ was reported. Generally, it is not surprising that even an interfacial layer with $R_{int} \sim 10^{-7}(m^2K)/W$ may preclude the beneficial effects of CNTs, as this may correspond to an interfacial thickness, t_{int} of the order of ~ 30 nm with $\kappa \sim 0.3$ W/(m K), i.e., through R_{int} $(= t_{int}/\kappa)$. Consequently, it can be inferred that the interface is (a) not confined to a bond length and/or (b) has a κ value smaller than that of the polymer matrix.

5 Conclusions

An investigation of heat transport characteristics in polymer composites, constituted of CNT fillers of two different aspect ratios, indicated a linear increase in the composite thermal conductivity proportional to the CNT volume fraction. There was a lack of predicted percolation behavior in the conductivity enhancement, as often observed in electrical conductivity measurements. In our used volume fractions (higher CNT filler content made the composites brittle), the CNTs do not form a percolation network due to the large interfacial thermal resistance with the polymer matrix. Consequently, CNTs, which have been posited to possess high thermal conductivity are effectively shielded and do not contribute significantly to the composite conductivity. The experimental data were fit satisfactorily through the use of an effective medium-based theory, considering the specific roles of the CNT and the interface in addition to the geometric parameters comprising the filler aspect ratio. Given the close correspondence of the determined interfacial resistance, R_{int}, to previous experiments and the reasonable value of $\kappa_{CNT} \sim 500$ W/(m K), we conclude that our experimental and modeling approaches can be used to study thermal transport behavior in nanotube–polymer composites.

Acknowledgment

We would like to thank Tom Chalfant and Isaiah Freerksen for help in fabrication of the setup. We are also thankful for insightful discussions with Prof. Renkun Chen, Max Aubain, Steve Pfeifer, Mark Hoefer, Robert Mifflin, and Byung-Wook Kim.

Nomenclature

κ = thermal conductivity
q = heat flux
t = thickness of sample being tested
T = temperature
CNT = carbon nanotube
R = thermal resistance
f = volume fraction
AR = aspect ratio of carbon nanotube
L = length of carbon nanotube
d = diameter of carbon nanotube
SWCNT = single-wall carbon nanotube
MWCNT = multiwall carbon nanotube

References

[1] Chung, D., 2001, "Comparison of Submicron-Diameter Carbon Filaments and Conventional Carbon Fibers as Fillers in Composite Materials," Carbon, **39**(8), pp. 1119–1125.
[2] Pfeifer, S., Park, S.-H., and Bandaru, P. R., 2010, "Analysis of Electrical Percolation Thresholds in Carbon Nanotube Networks Using the Weibull Probability Distribution," J. Appl. Phys., **108**(2), 15, p. 024305.
[3] Yu, C., Kim, Y. S., Kim, D., and Grunlan, J. C., 2008, "Thermoelectric Behavior of Segregated-Network Polymer Nanocomposites," Nano Lett., **8**(12), pp. 4428–4432.
[4] Park, S.-H., Theilmann, P. T., Asbeck, P. M., and Bandaru, P. R., 2010, "Enhanced Electromagnetic Interference Shielding Through the Use of Functionalized Carbon-Nanotube-Reactive Polymer Composites," IEEE Trans. Nanotechnol., **9**(4), pp. 464–469.
[5] Bigg, D. M., and Stutz, D. E., 1983, "Plastic Composites for Electromagnetic Interference Shielding Applications," Polym. Compos., **4**(1), pp. 40–46.
[6] Rashid, E. S. A., Ariffin, K., Akil, H. M., and Chee, C. K., 2008, "Mechanical and Thermal Properties of Polymer Composites for Electronic Packaging Application," J. Reinf. Plast. Compos., **27**(15), pp. 1573–1584.
[7] Narayana, S., and Sato, Y., 2012, "Heat Flux Manipulation With Engineered Thermal Materials," Phys. Rev. Lett., **108**, p. 214303.
[8] Shenogina, N., Shenogin, S., Xue, L., and Keblinski, P., 2005, "On the Lack of Thermal Percolation in Carbon Nanotube Composites," Appl. Phys. Lett., **87**(13), p. 133106.
[9] Landauer, R., 1978, "Electrical Conductivity in Inhomogeneous Media," AIP Conf. Proc., **40**(1), pp. 2–45.
[10] Huxtable, S., Cahill, D., Shenogin, S., Xue, L., Ozisik, R., Barone, P., Usrey, M., Strano, M., Siddons, G., Shim, M., and Keblinski, P., 2003, "Interfacial Heat Flow in Carbon Nanotube Suspensions," Nature Mater., **2**(11), pp. 731–734.
[11] Biercuk, M., Llaguno, M., Radosavljevic, M., Hyun, J., Johnson, A., and Fischer, J., 2002, "Carbon Nanotube Composites for Thermal Management," Appl. Phys. Lett., **80**(15), pp. 2767–2769.
[12] Bonnet, P., Sireude, D., Garnier, B., and Chauvet, O., 2007, "Thermal Properties and Percolation in Carbon Nanotube-Polymer Composites," Appl. Phys. Lett., **91**(20), p. 201910.
[13] Cahill, D. G., 1990, "Thermal Conductivity Measurement From 30 to 750 K: The 3 Omega Method," Rev. Sci. Instrum., **61**(2), pp. 802–808.

[14] Park, S.-H., and Bandaru, P. R., 2010, "Improved Mechanical Properties of Carbon Nanotube/Polymer Composites Through the Use of Carboxyl-Epoxide Functional Group Linkages," Polymer, **51**(22), pp. 5071–5077.
[15] ASTM Standard E1225, 2009, "Standard Test Method for Thermal Conductivity of Solids by Means of the Guarded-Comparative-Longitudinal Heat Flow Technique," ASTM International, West Conshohocken, PA, 2003, doi:10.1520/E1225-09, www.astm.org.
[16] ASTM Standard D5470, 2012, "Standard Test Method for Thermal Transmission Properties of Thermally Conductive Electrical Insulation Materials," ASTM International, West Conshohocken, PA, 2003, doi:10.1520/D5470-12, www.astm.org.
[17] Tleoubaev, A., Brzezinski, A., and Braga, L. C., 2008, "Accurate Simultaneous Measurements of Thermal Conductivity and Specific Heat of Rubber, Elastomers, and Other Materials," Proceedings of 12th Brazilian Rubber Technology Congress, Sao Paulo, Brazil, April 22–24.
[18] Price, D. M., and Jarratt, M., 2000, "Thermal Conductivity of PTFE and PTFE Composites," Proceedings of the Twenty-Eighth Conference of the North American Thermal Analysis Society, Orlando, FL.
[19] Bruggeman, D. A. G., 1935, "Berechnung Verschiedener Physikalischer Konstanten Von Heterogenen Substanzen," Ann. Phys. (Leipz.), **24**, p. 636.
[20] Balberg, I., 1985, "Universal Percolation-Threshold Limits in the Continuum," Phys. Rev. B, **31**, pp. 4053–4055.
[21] Deng, F., Zheng, Q.-S., Wang, L.-F., and Nan, C.-W., 2007, "Effects of Anisotropy, Aspect Ratio, and Nonstraightness of Carbon Nanotubes on Thermal Conductivity of Carbon Nanotube Composites," Appl. Phys. Lett., **90**(2), p. 021914.
[22] Swartz, E. T., and Pohl, R. O., 1989, "Thermal Boundary Resistance," Rev. Mod. Phys., **61**(3), pp. 605–668.
[23] Chen, T., Weng, G., and Liu, W., 2005, "Effect of Kapitza Contact and Consideration of Tube-End Transport on the Effective Conductivity in Nanotube-Based Composites," J. Appl. Phys., **97**(10, Part 1), p. 104312.
[24] Nan, C., 1994, "Effective-Medium Theory of Piezoelectric Composites," J. Appl. Phys., **76**(2), pp. 1155–1163.
[25] Nan, C., Birringer, R., Clarke, D., and Gleiter, H., 1997, "Effective Thermal Conductivity of Particulate Composites With Interfacial Thermal Resistance," J. Appl. Phys., **81**(10), pp. 6692–6699.
[26] Bryning, M. B., Milkie, D. E., Islam, M. F., Kikkawa, J. M., and Yodh, A. G., 2005, "Thermal Conductivity and Interfacial Resistance in Single-Wall Carbon Nanotube Epoxy Composites," Appl. Phys. Lett., **87**(16), p. 161909.
[27] Zhong, H., and Lukes, J. R., 2006, "Interfacial Thermal Resistance Between Carbon Nanotubes: Molecular Dynamics Simulations and Analytical Thermal Modeling," Phys. Rev. B, **74**(12), p. 125403.
[28] Nan, C., Li, X., and Birringer, R., 2000, "Inverse Problem for Composites With Imperfect Interface: Determination of Interfacial Thermal Resistance, Thermal Conductivity of Constituents, and Microstructural Parameters," J. Am. Ceram. Soc., **83**(4), pp. 848–854.
[29] Liang, Q., Moon, K.-S., Jiang, H., and Wong, C. P., 2012, "Thermal Conductivity Enhancement of Epoxy Composites by Interfacial Covalent Bonding for Underfill and Thermal Interfacial Materials in Cu/Low-K Application," IEEE Trans. Compon., Packag., Manuf. Technol., **2**(10), pp. 1571–1579.
[30] Liang, Q., Yao, X., Wang, W., Liu, Y., and Wong, C. P., 2011, "A Three-Dimensional Vertically Aligned Functionalized Multilayer Graphene Architecture: An Approach for Graphene-Based Thermal Interfacial Materials," ACS Nano, **5**(3), pp. 2392–2401.